Synthesis of novel diagnostic silicon nanoparticles for targeted delivery of thiourea to EGFR-expressing cancer cells

Mehrnaz Behray,[†] Carl A Webster,[‡,¥] Sara Pereira,[‡,¥] Paheli Ghosh,[§] Satheesh Krishnamurthy,[§] Wafa T. Al-Jamal,[‡] and Yimin Chao[†,*]

[†]School of Chemistry, University of East Anglia, Norwich NR4 7TJ, UK

[‡]School of Pharmacy, University of East Anglia, Norwich NR4 7TJ, UK

[§]Nanoscale Energy and Surface Engineering Department of Engineering and Innovation, The Open University, Buckinghamshire MK7 6AA, UK

KEYWORDS: silicon nanoparticles, epidermal growth factor, thiourea, imaging, colon cancer

ABSTRACT: The novel thiourea-functionalized silicon nanoparticles (SiNPs) have been successfully synthesized using allylamine and sulforaphane, an important anticancer drug, followed by a hydrosilylation reaction on the surface of hydrogen terminated SiNPs. Their physiochemical properties have been investigated by photoluminescence emission, FTIR and elemental analysis. MTT assay has been employed to evaluate in vitro toxicity in colorectal cancer cells (Caco-2) and primary normal cells (CCD). The results show significant toxicity of thiourea SiNPs after 72 h incubation in the cancer cell line and the toxicity is concentration dependent and saturated for concentrations above 100 µg/mL. Confocal microscopy images have demonstrated the internalization of thiourea-functionalized SiNPs inside the cells. Flow cytometry data has confirmed receptor-mediated targeting in cancer cells. This nanocomposite takes advantage of the EGFR active targeting of the ligand in addition to the photoluminescence properties of SiNPs for bioimaging purposes. The results suggest that this novel nanosystem can be extrapolated for active targeting of the receptors that are overexpressed in cancer cells such as EGFR using the targeting characteristics of thiourea-functionalized SiNPs and therefore encourage further investigation and development of anticancer agents specifically exploiting the EGFR inhibitory activity of such nanoparticles.

1. Introduction

Conventional cancer chemotherapies have been associated with serious systemic toxicities and dose-limiting side effects that limit their clinical application.[1] Targeted therapeutics on the other hand, by being more selective, can potentially minimize the side effects of these anticancer agents.[2-3] In efforts to develop targeted anticancer drugs, it is essential to consider many different aspects of molecular biology, such as the interactions with cell surface receptors.[4-5] Protein tyrosine kinases (PTKs) have been identified as major contributors in numerous signal transduction pathways within cell membranes and are implicated in cell proliferation.[6-7] Epidermal growth factor receptor (EGFR) kinase is one of the most important PTKs and plays a key role in a wide diversity of biological processes, including cell proliferation, metastasis, and angiogenesis.[8-10] Although EGFR is involved in various physiological processes, and as such is expressed in non-malignant tissues, this tyrosine kinase has been shown to be over-expressed in tumors of epithelial origin such as colon, breast, ovarian, lung, and prostate cancer.[11-12] Consequently, EGFR overexpression in cancerous tissue presents an attractive target for compounds with inhibitory activity.

Among the anticancer drugs discovered in recent years, thiourea compounds have shown potent anticancer properties owing to their strong inhibitory activity against receptor tyrosine kinases (RTKs), PTKs, and NADH oxidase which are all active in the process of tumorigenesis.[10-11, 13] Here, for the first time we report the synthesis of thiourea-functionalized silicon nanoparticles (SiNPs) as a new multifunctional nanoscale system. By developing such hybrid nanoparticles, we can exploit the unique optical properties of SiNPs whilst introducing the targeting characteristics of the thiourea ligand for diagnostic applications. One of the greatest challenges in nanomedicine, is defining the optimal targeting agents to selectively deliver nano-compounds to cancer tissues. Therefore, the capability of the targeting ligand to bind to the surface of the cancer cells is an important characteristic to trigger the receptor endocytosis. To this end, we herein report the synthesis and in vitro evaluation of the targeting and toxicity activities of thiourea-functionalized SiNPs. This approach investigates the ability of thiourea to target EGFR overexpression in cancer cells while taking advantage of the intrinsic photoluminescence properties of SiNPs, without the need for any fluorescent tags.

SiNPs are heavy metal free in nature and exhibit visible photoluminescence as a result of the quantum confinement effect.[14-17] The size tunable emission[18-20], high brightness[21], and high photostability compared to organic dyes[22], have made SiNPs attractive materials as fluorescent cellular markers. In addition, silicon is abundant and economical[23] but more importantly silicon has low inherent toxicity. Studies report silicon to be almost ten times safer than cadmium-based counterparts for use in biomedical and bioimaging applications.[24] Unlike other semiconductors, silicon has an indirect band gap

that provides significant optical properties due to their very small size (about 4 nm), which is close to the bulk Bohr radius.[20, 25]

SiNPs have been prepared by a variety of physical and chemical approaches utilizing top down and bottom up techniques such as electrochemical etching,[26-27] thermal vaporization,[28] ion implantation,[29] gas phase decomposition of silanes,[30-31] and laser ablation.[32] Bottom up techniques of preparing NPs in solutions can simultaneously offer the control over the surface chemistry and particle size.[33] However, consideration of the challenges regarding sample purification is more important in terms of the biomedical applications. Thus, top down techniques such as electrochemical etching might be favourable in this regards to provide SiNPs with high purity.[34]

In the present study, a thiourea ligand was synthesized followed by hydrosilylation to functionalize SiNPs with this specific functional group. The hydrogen terminated SiNPs were first prepared through the electrochemical etching of porous silicon and later functionalized by thiourea. These functionalized SiNPs were tested in terms of cytotoxicity to colorectal cancer and primary cells and active EGFR-mediated targeting. In several respects, these novel nanoparticles offer significant advantages compared to conventional therapeutics. These include the integration of the targeting moiety and therapeutic moiety in the same system, the use of inexpensive materials and more importantly the production of a highly stable nanosystem.

2. Experimental Methods

2.1 General procedure for synthesis of thiourea-functionalized SiNPs

Hydrogen terminated SiNPs were synthesised by galvanostatic anodization of porous Silicon layer (boron-doped p-Si (100) chip with 1.25 × 1.25 cm^2 size) in a 1:1 v/v solution of 48% aqueous HF and ethanol as reported previously.[27]

Thiourea chain was obtained after 6 hrs refluxing of sulforaphane (4 µl, 0.0225 mmol) with 2 equivalent of allylamine (3.37 µl, 0.45 mmol) at RT in dry acetone under N_2. The product was reacted with hydrogen terminated SiNPs obtained from etching of 4 Silicon chips for extra 24 hours in EtOH at 35 ºC as described in Scheme 1. The mixture solution was centrifuged and the solvent was evaporated under the reduced pressure at 60 ºC. 20 mg of thiourea-functionalized SiNPs was obtained from each batch.

2.2 Chemical characterization

Fourier transform infrared spectroscopy (FTIR) Measurements were carried out using a Perkin-Elmer ATR-FTIR spectrometer from the solid sample of thiourea-functionalized SiNPs. The spectra were recorded after 16 scans by correcting the background.

X-ray photoelectron spectroscopy (XPS) measurements were performed on a K-Alpha XPS instrument (Thermo Scientific, East Grinstead, UK) at NEXUS. A few drops of the suspension of thiourea-functionalized SiNPs in EtOH were cast onto a cleaned gold substrate. The film was introduced into a load-lock attached to ultra-high vacuum (UHV) chamber in which the typical pressure was maintained below 5 × 10^{-9} mbar. All spectra were acquired at normal emission with AlKα radiation at 1486.6 eV and a spot size of 400 µm. A pass energy of 200 eV and step size of 0.4 eV was used for the survey spectra and a pass energy of 40 eV and step size of 0.1 eV was used for high resolution spectra. In all photoemission spectra, binding energies (BEs) were referred to the Au $4f_{7/2}$ line measured on a gold foil in direct electrical contact with the sample which was found at binding energy of 84 eV.

2.3 Particle size analysis and stability

Transmission electron microscopy (TEM) studies were performed with the JEOL, JEM 2100 microscope running a LaB6 (lanthanum hexaboride crystal) emitter at voltage 200 kV. TEM samples were prepared by drop-casting a dilute suspension of the sample dispersed in EtOH onto a 200 mesh carbon-coated copper grid. The grids were dried before the measurement. TEM micrographs were taken at different spots of grids.

The hydrodynamic diameter of thiourea-functionalized SiNPs and polydispersity index were determined by dynamic light scattering (DLS) measurement with Zetasizer Nano ZS (Malvern Instruments Ltd, UK) at room temperature, equilibrating samples for 120 seconds prior to the measurement. 1 mg/mL of thiourea-functionalized SiNP solution was measured in distilled water and PBS, as well as RPMI and complete RPMI (supplemented with 10% FBS) media to assess the stability of the thiourea-functionalized SiNPs under *in vitro* conditions. Size measurements were performed in triplicates. Zeta potential was measured using the above protocol in water in the same instrument.

2.4 Optical Characterization

UV-Vis absorption (UV-Vis) and Photoluminescence (PL) spectroscopy were performed on thiourea-functionalized SiNPs dispersed in EtOH. The UV-Vis absorption spectra of thiourea-functionalized SiNPs were recorded by a PerkinElmer 35 UV-vis double-beam spectrometer in a quartz cuvette (10×10 mm). The scan range was over a 300 to 700 nm at a rate of 900 nm/min and the spectra were corrected by subtracting the background contribution from the dispersing solvent.

The PL spectra were collected using a Perkin Elmer LS55 spectrometer in a quartz cuvette (10×10 mm). The excitation wavelength was fixed at 340 nm with the excitation and emission slit widths set at 10 nm. The emission spectra were corrected by the background spectra which was from the solvent emission.

2.5 Cell culture

Caco-2 (human colorectal adenocarcinoma) and CCD-841 (human normal colon epithelial) cells were a kind gift from Dr Yongping Bao (Norwich Medical School, UK). Cells were sub-cultured in RPMI supplemented with 10% fetal bovine serum, 2 mM L-glutamine, 100 µg/mL penicillin, and 100 µg/mL streptomycin (Life Technologies, Carlsbad, CA) and maintained in a humidified incubator at 37 ºC within an atmosphere containing 5% CO_2. Both cells tested negative for mycoplasma.

2.6 Cytotoxicity

Cytotoxicity of thiourea-functionalised SiNPs was assessed by standard MTT assay.[35] Caco-2 and CCD cells were seeded in a 96-well culture plate at a seeding density of 4.5×10^4 cells per well. After 24 h the media was removed and replaced with a range of different concentrations of NPs suspension from 5 to 1500 µg/mL for 24 and 72 h. The absorbance was measured using BMG Labtech Polar Star Optima microplate reader at 570 nm. Percentage of viable cells was calculated from a minimum of triplicate wells and normalized to untreated control cells. Results were expressed as mean ± SD of at least three independent experiments.[36]

2.7 Cellular internalization by Laser scanning confocal microscopy

Caco-2 cells were seeded on a 12-well plate with glass cover slips. Next day, cells were incubated with 100 µg/mL of thiourea-functionalized SiNPs for 4 hours. Cells were washed and fixed with 4% (v/v) paraformaldehyde (PFA) (Sigma-Aldrich) in PBS solution for 20 min at room temperature. Nuclei were stained with Hoechst 33342 (Sigma-Aldrich) (2 µg/mL) in PBS for 5 min. Actin was stained using Texas Red-X Phalloidin (Life Technologies) (6.6 µM). Laser scanning confocal microscopy was performed on a Zeiss LSM510 META confocal microscope using a 63 × oil immersion objective lens for imaging. Laser beams with 364, 488 and 543 nm excitation wavelengths were used to image nuclei, SiNPs and actin respectively.

2.8 Flow cytometry

Caco-2 and CCD cells were seeded on 24 well plates at a density of 5×10^4 cells per well and treated with thiourea and amine capped SiNPs at a concentration of 100 µg/mL from 30 minutes to 8 hours. The cells were trypsinized and then washed three times with PBS followed by centrifugation at 1200 rpm for 5 min after each washing. Cells were fixed with 4% (v/v) PFA in FBS for 20 min and washed again with PBS. Prior to the flow cytometric measurement, the cells were re-suspended in a buffer of 5 % (v/v) FBS in PBS. The uptake of NPs was examined in 10,000 gated cells by detecting SiNPs fluorescence using FL1 channel detector and a BD FACSCalibur (BD Bioscience). Measurements were performed in triplicate (with different sets of NPs) and data was analyzed with CellQuest Pro® software (BD Biosciences) and presented as median ± SD.

2.9 Statistical analysis

Statistical methods throughout this study are represented as mean ± SEM taken over a minimum of three independent experiments. Statistical significance was measured by two-way-ANOVA followed by a Bonferroni post-test using GraphPad Prism version 5.03 for Windows, GraphPad Software, San Diego California USA.

3. Results and discussion

3.1 Synthesis of thiourea-functionalized SiNPs

Conjugation of thiourea onto SiNPs has high potential for the active targeting of EGFR overexpressing cancer cells. This can therefore increase the stability of silicon, enhance the nanoparticle cell uptake and reduce the fast clearance of the nanoparticles from the body since the capping ligand renders hydrogen terminated SiNPs hydrophilic to provide stable dispersions. In order to evaluate the potential of such systems, a ligand containing a thiourea segment was synthesized via the reaction between sulforaphane and allylamine and subsequently used to functionalize the surface of hydrogen terminated SiNPs obtained from the electrochemical top down method as previously described (Scheme 1).

3.2 Fourier transform infrared spectroscopy (FTIR)

The FTIR spectra of Sulforaphane, thiourea and thiourea-functionalized SiNPs are presented in Fig. 1. Absorption peak at 1012 represents S=O in the structure of Sulforaphane as the starting material. Vibrations related to C-N and C-S bonds can be seen at 1298 and 692 cm^{-1} respectively.[37-38] The characteris-

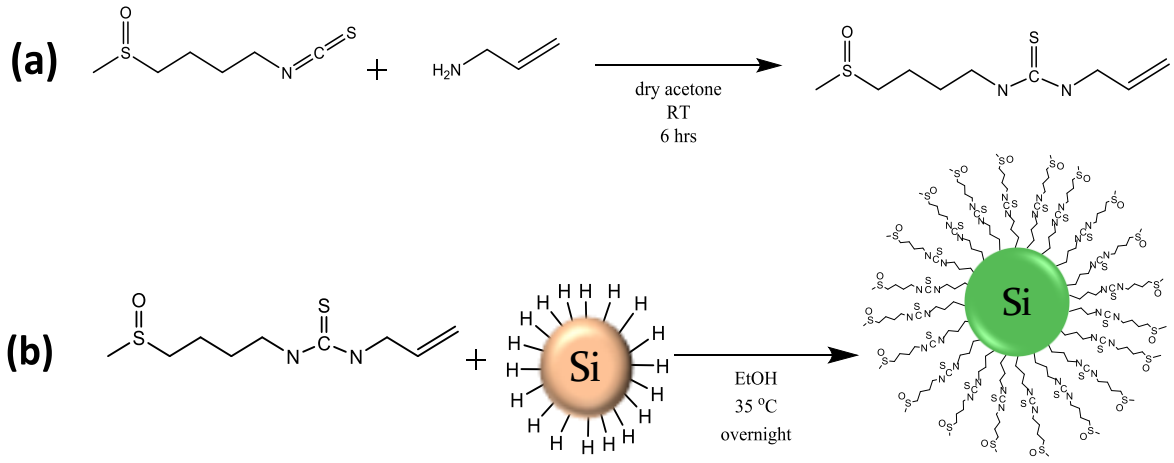

Scheme 1. Schematic illustration of (a) the chemical synthesis of thiourea ligand and (b) the conjugation of thiourea onto the surface of hydrogen capped silicon nanoparticles via hydrosilylation reaction.

tic feature of isothiocyanate functional group can be clearly observed as a prominent double peak at 2099 cm^{-1}.[39] These peaks disappeared after reacting with allylamine but the stretching frequencies related to N-C-N vibrations in thiourea group were found at 1545 cm^{-1}. The band at 3279 cm^{-1} represent the stretching vibration of the N-H bond in the derivative thiourea.[40] After surface functionalisation of SiNPs with thiourea, a peak at 1258 cm^{-1} can be seen which is a strong indicator of Si-C bonding.[41] In addition, there was no evidence of Si-H stretching at 2100 cm^{-1}.[16] Therefore, the thiourea ligand with a terminal double bond reacted with the hydrogen terminated silicon surface via hydrosilylation in order to give a covalent Si-C linkage on the surface of the nanoparticles.

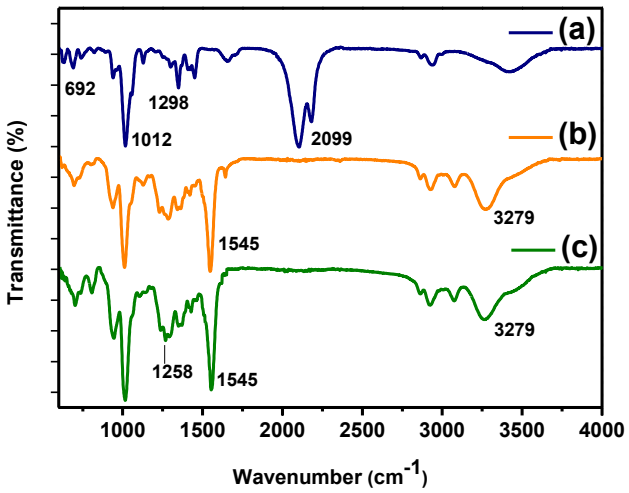

Fig. 1 FTIR spectra of (a) sulforaphane; (b) thiourea and (c) thiourea-functionalized SiNPs. The relevant features of each spectrum are highlighted.

3.3 X-ray photoelectron spectroscopy (XPS)

For further evidence of the nanoparticle structure, the surface chemical bonding was investigated using the full survey and high resolution XPS spectroscopy. Fig. 2a shows the full survey of the photoelectron spectrum. The high resolution XPS spectra of Si2p, C1s, O1s and N1s regions taken on a thin film of thiourea-functionalized SiNPs are presented in Fig. 2b to e. Fig. 2b indicates that the Si2p spectrum is fitted with three components and a Shirley background. The three peaks are located at 101.95, 102.73 and 100.91 eV. The first peak is attributed to Si-C confirming the hydrogen on the surface of SiNPs is replaced with thiourea.[34] The second peak at binding energy 102.73 eV is related to Si-O due to partial surface oxidation under the ambient conditions.[42] The third component at 100.91 eV is assigned to Si-Si within silicon core of NPs.[43-44] The C1s spectrum is fitted with three components and a Shirley background, see Fig. 2c. The four peaks are appeared at 284.65, 284.04, 285.50 and 286.72 eV. The first component at 284.65 eV is attributed to C-C bonding. The second peak at 284.04 eV related to the existence of C-Si and finally the last two peaks at 285.50 and 286.72 eV are assigned to C-H and C-N respectively.[45-46] The O1s spectrum is presented in Fig. 2d and fitted with three components and a Shirley background. The first peak is related to partial oxidation at 532.01 eV for Si-O. The second binding energy at 533.25 eV is attributed to some hydroxide O-H group. The last component of O1s spectrum is assigned to O-S at 531.10 eV.[44] The N1s spectrum is presented in Fig. 2e and fitted with two components and a Shirley background. The peak at 399.58 eV is assigned to C-N bonding in the thiourea. The other peak at 398.67 eV is attributed to N-C=S.[47] According to the surface chemistry data obtained from XPS the surface of SiNPs is fully capped with the ligand. A table with the quantification of XPS data can be seen in Table S1 in the supporting information.

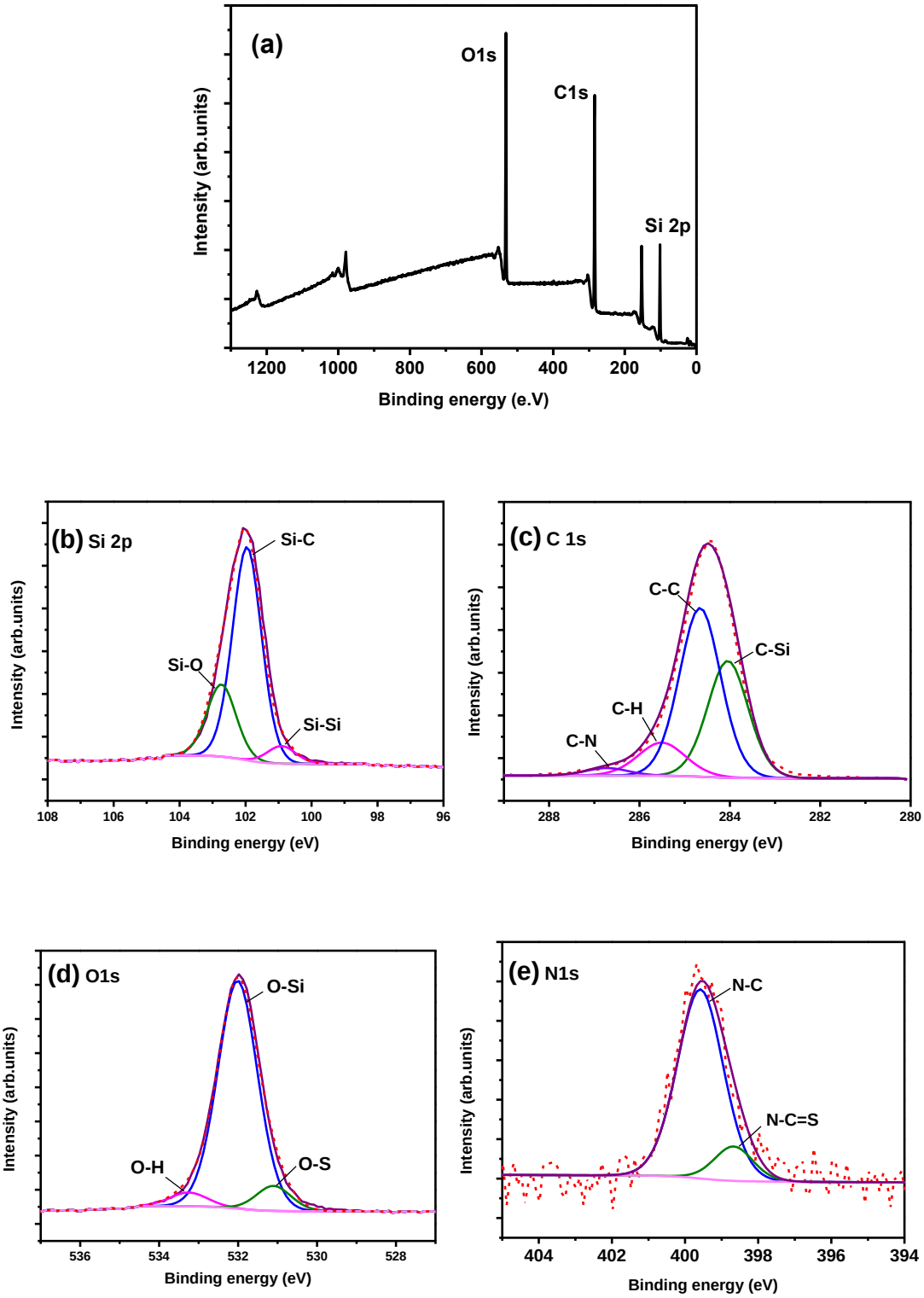

Fig. 2 XPS spectra obtained from thiourea-functionalized SiNPs. (a) Full survey (b) Si2p (c) C1s (d) O1s (e) N1s. The dotted lines are experimental data that are fitted with different components.

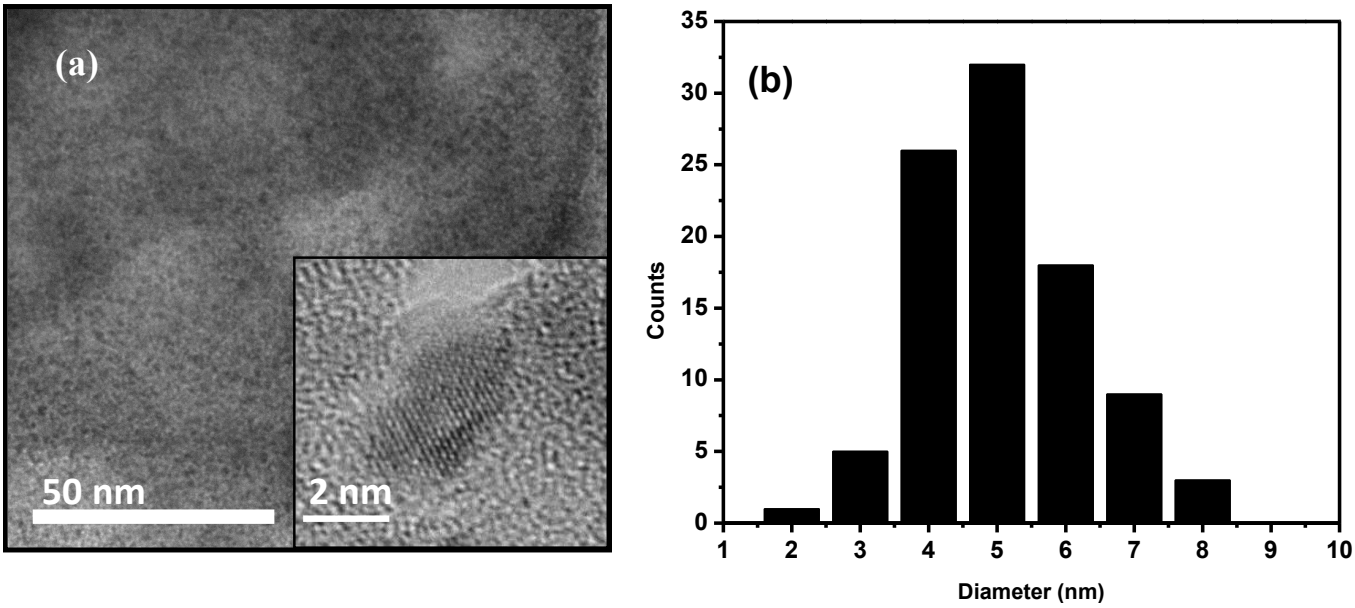

Fig. 3 (a) TEM image of thiourea-functionalized silicon nanoparticles. The insert shows an enlarge view of the high resolution image of the crystalline structure. (b) the corresponding histogram of nanoparticle size distribution after analyzing 88 particles.

Table 1 Mean hydrodynamic diameters and zeta potential of thiourea-functionalized SiNPs measured by DLS in different media.

Solvent	Mean particle Size (nm) ± SD	Polydispersity index ± SD	Zeta potential (mV) ± SD
Water	11.32 ± 1.30	0.16 ± 0.05	21 ± 0.80
PBS	12.20 ± 1.05	0.22 ± 0.05	NA
RPMI	12.50 ± 1.26	0.20 + 0.10	NA
RPMI/10% FBS	16.70 ± 4.08	0.33 ± 0.04	NA

3.4 Size measurement and stability

Fig. 3a illustrates a TEM image of thiourea-functionalized SiNPs on a carbon coated copper grid. A mean size and size distribution was found to be 4.5 nm after analyzing approximately 100 SiNPs from different regions of the grid. (Fig. 3b) The insert figure shows the crystalline structure of the individual NPs. The mean hydrodynamic diameters of thiourea-functionalized SiNPs are represented in Table 1, in different solvents: water, PBS as well as the cell culture media RPMI and RPMI/10% FBS. According to the data, SiNPs show almost the same average diamaters in all solvents. This is more than double than the core size of SiNPs due to the formation of an outer shell after the interaction between the capping ligand and the surrounding environment.[48] However, the average diameter and the polydispersity index (PDI) are slightly increased for NPs in the RPMI containing 10% FBS, suggesting the expected adsorption of serum proteins on the surface of positively-charged SiNPs. This is because of the small size of SiNPs and their large surface area which lead to partial aggregation in the biological media, and therfore the presence of protiens reduces the surface energy. Nevertheless, the aggregation was not significant as the main population of the SiNPs was still observed around the expected sizes similar to other solvents less than 20 nm. The Zeta potential of NPs was measured in water and found to be 21 ± 0.80 mV. The surface charge of thiourea-functionalized SiNPs was tested in human plasma to investigate the effect of protein adsorption on Zeta potential values of NPs (see Fig. S1 in supporting information).

3.5 Absorption and luminescence spectroscopy

Absorption and emission spectra of thiourea-functionalized SiNPs are presented in Fig. 4. The inset photograph is the sample under UV illumination at 254 nm. NPs were dispersed in EtOH prior to the measurement as this improved the solubility of the sample. The gradual increase in the absorbance with decreasing excitation wavelength from the onset wavelength of 430 nm, corresponding to the absorption edge of 2.88 eV, is characteristic of absorption across the indirect band gap of silicon.[23] The solid line shows the photoluminescence spectrum of thiourea-functionalized SiNPs with the maximum emission peak centre at approximately 420 nm and a full width at half-maximum height (FWHM) of 79 nm under an excitation wavelength of 340 nm.

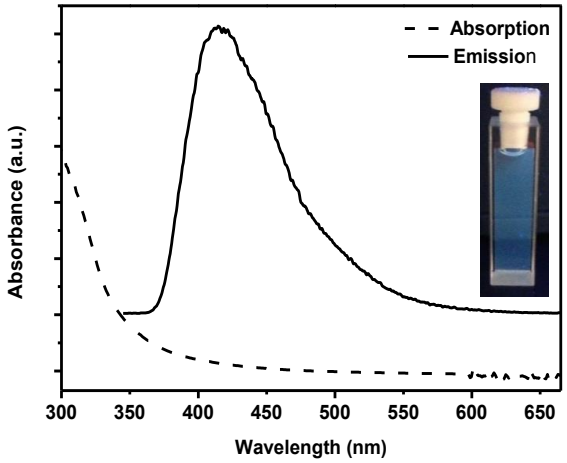

Fig. 4 Absorption and emission spectra of thiourea-functionalized SiNPs at excitation at 340 nm. The inset image shows the fluorescence from a vial of sample in EtOH when excited with a UV lamp.

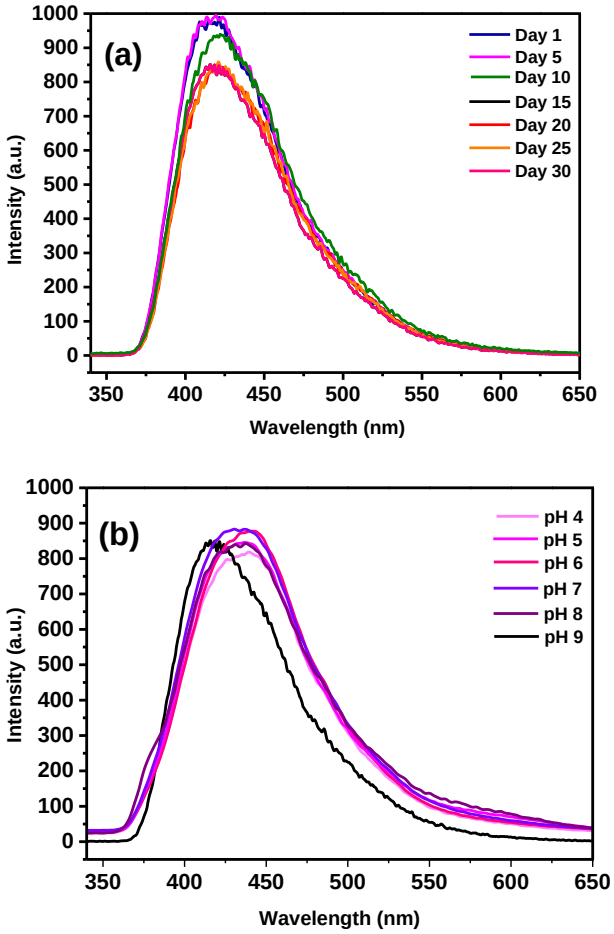

Fig. 5 (a) Long term PL stability of thiourea-functionalized SiNPs stored in EtOH. (b) PL stability of thiourea-functionalized SiNPs in buffers of different pH values.

A fluorescence quantum yield (QY) of 9.94% was measured by a comparative method described by Williams et al,[49] using quinine sulphate in 0.1 M H_2SO_4 as reference (Fig. S2).

In order to have a more efficient system in terms of biomedical applications, it is important to obtain NPs with suitable PL stability. The long term stability of the synthesized SiNPs in EtOH was tested over a month and it was found that NPs can maintain about 80% of their initial PL after 30 days (Fig. 5a). The stabilization of the PL by the coating ligand is attributed to the covalent passivation of the surface by the thiourea which can prevent the oxidation of the NP surface.

The pH is a fundamental parameter for biomedical uses, and thus the PL stability of thiourea-functionalized SiNPs was tested over a range of different pH values. Fig. 5b represents the changes in the intensity and peak wavelength of SiNPs in various pH values from 4 to 9. Based on the data obtaied, the photoluminescence intensity was stable over a range of physiologically relevant pH environment. Additionally, for pH levels 4-8 the peak position of the maximum PL emission remained unchanged, however for the most alkali pH 9 this shifted slightly to a lower wavelength (see Fig. S3) This indicates the role of the inorganic capping ligand to isolate the silicon core from the surrounding environment and thereore makes SiNPs suitable for further biomedical investigations.

3.6 Cytotoxicity assay by MTT

Modifying the surface chemistry of NPs, given their large surface area, alters the toxicity and biological characteristics which can be beneficial for biomedical applications. In this study, the cytotoxicity of thiourea-functionalized SiNPs in colon cancer cells and their equivalent normal cell line is evaluated by MTT assay. Amine-functionalized SiNPs, which have been identified as a non-toxic biomaterial,[50] were used in this project as a control compound. Cells were exposed to increasing concentrations ranging from 5 to 1500 µg/mL thiourea and amine-functionalized SiNPs. After 24 hours incubation, a MTT assay was carried out in Caco-2 and CCD cells and the absorbance values were normalized to the untreated cells. The results indicate that for the NPs used in the current study, concentrations up to 1500 µg/mL did not show any significant toxicity after 24 h incubation (Fig. 6a and b). For this time point, both thiourea and amine- functionalized SiNPs reduced CCD and Caco-2 cell viability by approximately 20-25%, which indicates that the anticancer activity of thiourea did not develop in this short incubation time. In Caco-2 cells, thiourea-functionalized SiNPs had a slightly larger effect than amine-functionalized SiNPs for concentrations around 50 µg/mL. For the longer 72 hours exposure (Fig. 6c and d), the Caco-2 cell viability dropped by 60% for concentrations above 100 µg/mL, a result that was not reproduced by amine-functionalized SiNPs which had negligible effect beyond 24 hours. Lower cell viability was observed at lower concentrations of thiourea-functionalized SiNPs in Caco-2 cells than in CCD, which is important if the treatment is to be effective whilst having a less impactful effect on normal cells. In CCD cells the behaviour was similar for both thiourea and amine-functionalized SiNPs.

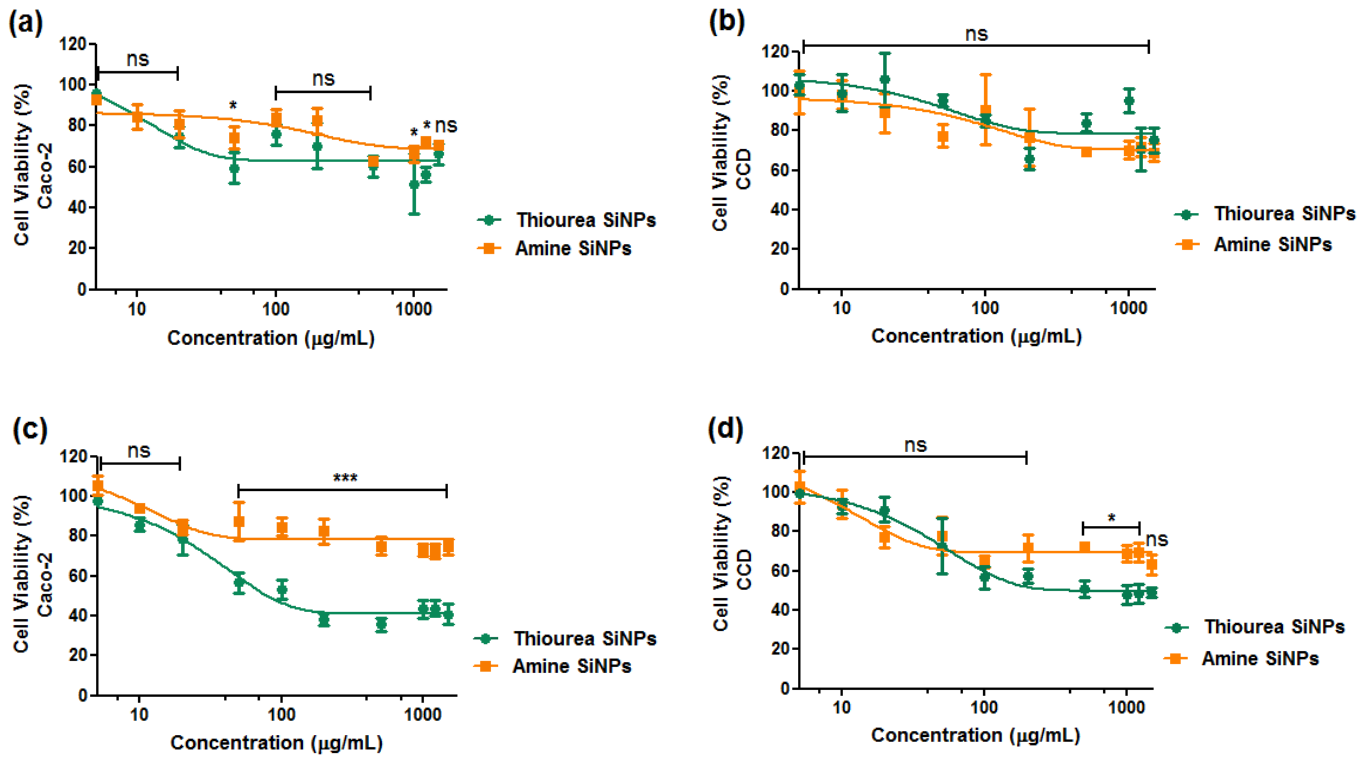

Fig. 6 *In vitro* cytotoxicity of thiourea and amine capped SiNPs by MTT after incubation with Caco-2, 24 h (a), CCD,24 h (b), Caco-2, 72 h (c) and CCD for 72 h incubation (d) at 37 ºC. (The results were normalized to non-stimulated cells.) Statistical significance was determined by two-way-ANOVA followed by a Bonferroni post-test. (*P < 0.05, ***P < 0.001, ns statistically not significant). Results are expressed as mean ± SEM (n =3).

The high dosage of nanoparticles to be effective in this case may not seem to be appropriate (1500 µg/mL), however, it should be mentioned that the concentration used for the MTT assay is calculated with the whole entity of functionalized SiNPs, i.e. drug with the covalently bonded silicon core and based on the TGA data shown in the supporting information (Fig. S4) almost 60 % on the concentration is attributed to the silicon. Therefore, for thiourea-functionalized SiNPs to be more effective in terms of the cytotoxic effects, a higher dose of nanoparticles is needed (more than 100 µg/mL). In addition, the low intrinsic toxicity of silicon in nature, would make the application of SiNPs at such high dosage possible as there would be not much concern regarding the safety of silicon used in these multifunctional nanomaterials.

3.7 Cellular uptake studies

In order to understand the uptake behaviour of thiourea-functionalized SiNPs at the cellular level, the cellular internalization and intercellular distribution of NPs were evaluated by confocal imaging. Fig. 7 shows the confocal images of Caco-2 cells incubated with 100 µg/mL of thiourea-functionalized SiNPs for 4 h at 37 ºC compared to untreated control cells. Based on the images obtained, thiourea-functionalized SiNPs were successfully internalized within the cell cytoplasm as shown by the green fluorescence. For further evidence of the internal distribution of SiNPs, Z-stack images are shown in supplementary information (Fig. S5).

3.8 Flow cytometry

For additional SiNP uptake evidence, flow cytometry was used in both cancer and normal cells to semi-quantitavely measure cellular uptake of the NPs (see Fig. 8).

The two well-known cell lines, Caco-2 and CCD-841, were chosen because of their different expression of EGFR. In literature, Caco-2 cells have been shown to overexpress the EGFR mRNA to almost 5 fold when normalized to the CCD cells as control, while CCD cells did not show EGFR overexpression and lacked observable EGFR phosphorylation.[51]

Thiourea and amine-functionalized SiNPs (each 100 µg/mL) were incubated with both cells (Caco-2 and CCD) for five different time periods (from 30 min to 8 h). Median fluorescence values demonstrate cell uptake of thiourea and amine-functionalized SiNPs. The data has confirmed considerably more uptake of thiourea-functionalized SiNPs in Caco-2 cells compared to amine-functionalized SiNPs for all time points (Fig 8a). Moreover, the fluorescent signal of thiourea-functionalized SiNPs increased gradually between 30 min and 4 h. At 4 h exposure the maximal thiourea-functionalized SiNP uptake was observed, where longer time (6 and 8 h) did not increase the cellular uptake. This suggests that thiourea-

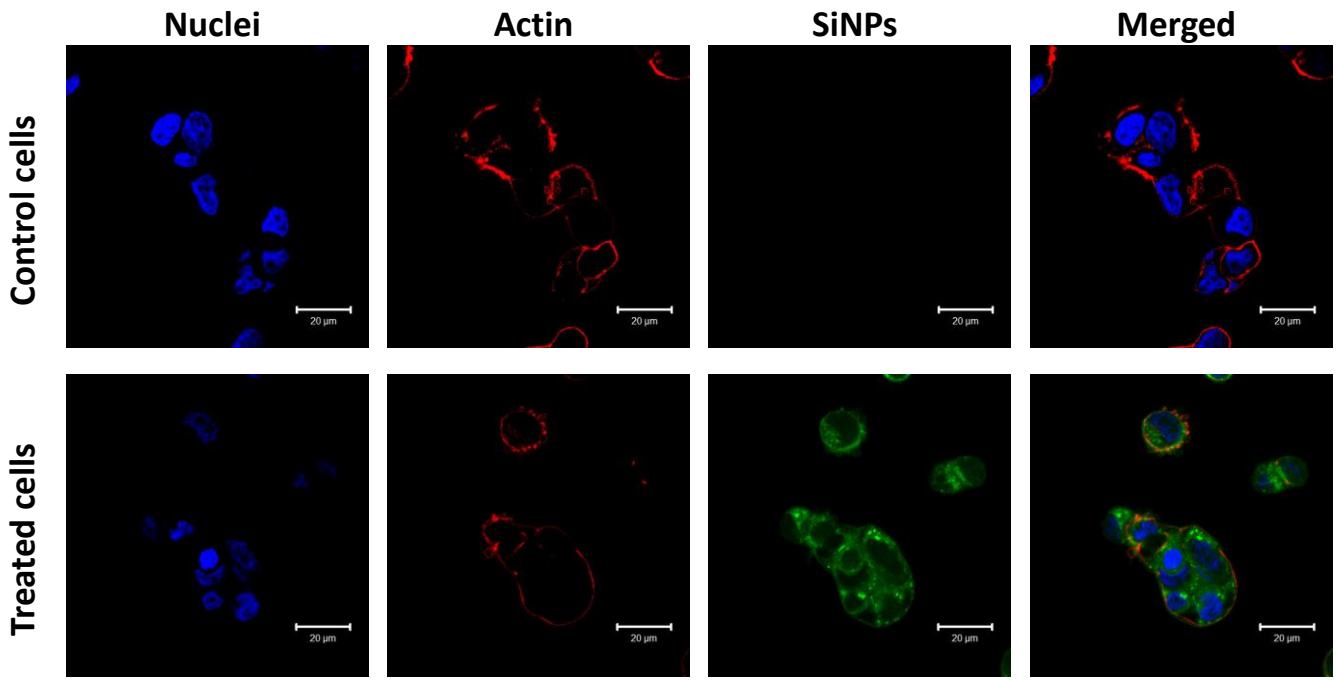

Fig. 7 Confocal fluorescence images of Caco-2 cells incubated with thiourea capped SiNPs for 4 h compared to control (untreated) cells (top row). Blue from Hoechst for nuclei, red from Phalloidin for actin staining and green fluorescence from thiourea capped SiNPs.

functionalized SiNPs reached an uptake saturation level, whereas the non-specific cellular uptake of amine-functionalized SiNPs increased overtime. A plausible explanation for this result, consistent with previous known characteristics of thiourea-functionalized SiNPs, is that the thiourea-functionalized SiNP uptake mechanism is through the receptor-mediated endocytosis by the interaction with EGFR as the cell internalization in this case can occur within the early hours of receptor stimulation.[52] Amine-functionalized SiNPs on the other hand have no known similar interaction, and thus the lower levels of internalization are reached through passive, rather than active targeting. Since a saturation level was reached for thiourea-functionalized SiNPs, it is more likely that EGFR are transported to endosome/lysosome for degradation rather than the possibility of the receptor recycling process which would lead to the increase of uptake overtime.[53] The introduction of thiourea-functionalized SiNPs in cancer cells therefore can potentially manage the multiple cellular processes in which EGFR is a key player and thus an inhibit tumour growth. However, the level of thiourea-functionalized SiNP uptake in CCD cells seemed to be much lower (Fig. 8b). A higher florescence was observed at the shorter time point of 1 h incubation. For longer incaution times, up to 8 h exposure, the uptake decreased.

One possible explanation for this behaviour could be that the presence of the ligand caused some steric alteration which reduced the uptake of thiourea- SiNPs for longer exposure. This may be compounded by the fact that expression of EGFR in primary epithelial colon cells is less than cancer cells.[54]

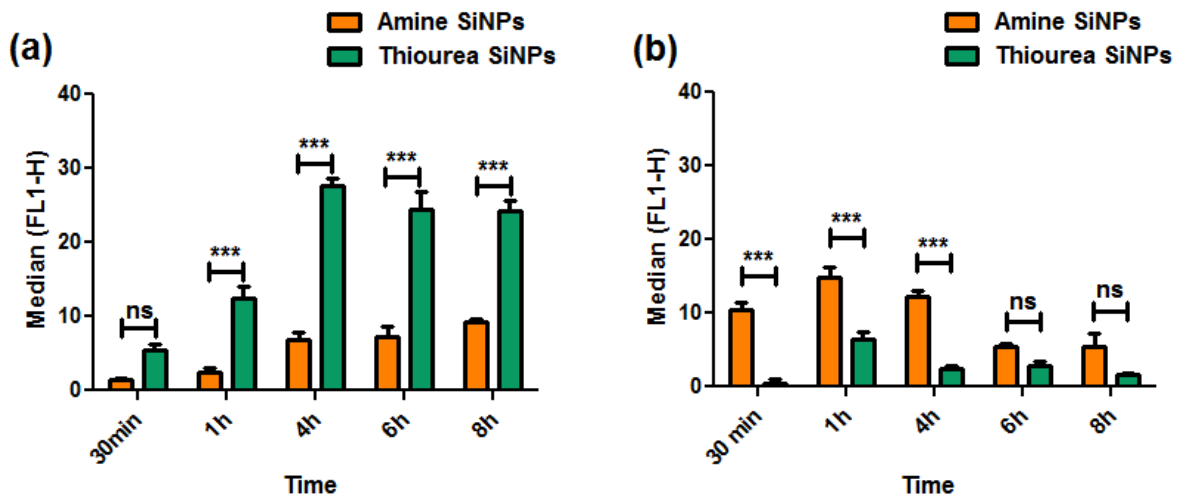

Fig. 8 Flow cytometric analysis of the thiourea and amine-functionalized SiNPs in (a) Caco-2 and (b) CCD cells showing the time dependent behavior of uptake. Statistical significance was determined by two-way-ANOVA followed by a Bonferroni post-test. (***P < 0.001, ns statistically not significant). Results are expressed as mean ± SEM (n =3).

4. Conclusions

We reported here the synthesis of thiourea-functionalized SiNPs as a novel nanodelivery system, which can be actively targeted towards cancer cells that over express of EGFR. This approach makes use of the physiochemical and biological properties of both components of the nanosystem, in particular the photoluminescence of SiNPs and the anticancer activity of thiourea. According to the FTIR and elemental analysis, SiNPs are fully capped with the thiourea ligand. The stability of SiNPs in different biological media, as a result of the covalent conjugation of the ligand on the surface of nanoparticles, was shown by DLS. This result has addressed the challenges regarding the long term stability of nanoparticles for similar biomedical applications. The in vitro toxicity of the novel nanoparticles was verified by MTT assay in colorectal cancer and normal cells. The thiourea-functionalized SiNPs were shown to be toxic after 72 hours exposure to the cancer cells. Considering the data obtained from uptake studies in both Caco-2 and CCD cells, it was shown that thiourea-functionalized SiNPs were distributed within the cytoplasm as visualized in confocal images. The uptake of thiourea-functionalized SiNPs was found to show a time dependent behavior. The fluorescent signal increased gradually between 30 min and 4 h. The saturation uptake level suggested the ligand binds with the receptor and therefore the degradation of EGFR after 4 hours is most likely to occur. This is significant in term of developing future diagnostic tools for drug delivery systems. Overall, the nanodelivery system developed herein presents an encouraging platform for drug delivery particularly aiming for the targeting of EGFR overexpression in cancer cells.

SUPPORTING INFORMATION

Synthesis of amine terminated SiNPs, Stability in human plasma including zeta potential of SiNPs in human plasma at different time points, Quantum Yield measurements, PL stability in different pH buffer, TGA analysis with the spectra showing TGA and derivative of SiNPs, Z-stack confocal imaging, data from Elisa assay, and the XPS fitting data. This material is available free of charge via the Internet at http://pubs.acs.org.

AUTHOR INFORMATION

Corresponding Author

*E-mail: y.chao@uea.ac.uk.

Author Contributions

The manuscript was written through contributions of all authors. / All authors have given approval to the final version of the manuscript. / ¥ These authors contributed equally. (match statement to author names with a symbol)

ACKNOWLEDGMENT

MB is grateful to an International studentship awarded by the University of East Anglia.
X-ray photoelectron spectra were obtained at the National EPSRC XPS Users' Service (NEXUS) at Newcastle University, an EPSRC Mid-Range Facility.

REFERENCES

(1) Peer, D.; Karp, J. M.; Hong, S.; FaroKhzad, O. C.; Margalit, R.; Langer, R., Nanocarriers as an Emerging Platform for Cancer Therapy. *Nat. Nanotechnol.* **2007,** *2* (12), 751-760.

(2) Allen, T. M., Ligand-Targeted Therapeutics in Anticancer Therapy. *Nat. Rev. Cancer* **2002,** *2* (10), 750-763.

(3) Davis, M. E.; Chen, Z.; Shin, D. M., Nanoparticle Therapeutics: An Emerging Treatment Modality for Cancer. *Nat. Rev. Drug Discovery* **2008,** *7* (9), 771-782.

(4) Hynes, N. E.; Lane, H. A., Erbb Receptors and Cancer: The Complexity of Targeted Inhibitors. *Nat. Rev. Cancer* **2005,** *5* (5), 341-354.

(5) Sinha, R.; Kim, G. J.; Nie, S. M.; Shin, D. M., Nanotechnology in Cancer Therapeutics: Bioconjugated Nanoparticles for Drug Delivery. *Mol. Cancer Ther.* **2006,** *5* (8), 1909-1917.

(6) Ullrich, A.; Schlessinger, J., Signal Transduction by Receptors with Tyrosine Kinase-Activity. *Cell* **1990,** *61* (2), 203-212.

(7) Lynch, T. J.; Bell, D. W.; Sordella, R.; Gurubhagavatula, S.; Okimoto, R. A.; Brannigan, B. W.; Harris, P. L.; Haserlat, S. M.; Supko, J. G.; Haluska, F. G.; Louis, D. N.; Christiani, D. C.; Settleman, J.; Haber, D. A., Activating Mutations in the Epidermal Growth Factor Receptor Underlying Responsiveness of Non-Small-Cell Lung Cancer to Gefitinib. *N. Engl. J. Med.* **2004,** *350* (21), 2129-2139.

(8) Carpenter, G., Receptors for Epidermal Growth-Factor and Other Polypeptide Mitogens. *Annu. Rev. Biochem* **1987,** *56*, 881-914.

(9) Salomon, D. S.; Brandt, R.; Ciardiello, F.; Normanno, N., Epidermal Growth Factor-Related Peptides and Their Receptors in Human Malignancies. *Crit. Rev. Oncol. Hematol.* **1995,** *19* (3), 183-232.

(10) Li, J.; Tan, J.-z.; Chen, L.-l.; Zhang, J.; Shen, X.; Mei, C.-l.; Fu, L.-l.; Lin, L.-p.; Ding, J.; Xiong, B.; Xiong, X.-s.; Liu, H.; Luo, X.-m.; Jiang, H.-l., Design, Synthesis and Antitumor Evaluation of a New Series of N-Substituted-Thiourea Derivatives. *Acta Pharmacol. Sin.* **2006,** *27* (9), 1259-1271.

(11) Lv, P.-C.; Li, H.-Q.; Sun, J.; Zhou, Y.; Zhu, H.-L., Synthesis and Biological Evaluation of Pyrazole Derivatives Containing Thiourea Skeleton as Anticancer Agents. *Biorg. Med. Chem.* **2010,** *18* (13), 4606-4614.

(12) Herbst, R. S., Review of Epidermal Growth Factor Receptor Biology. *Int. J. Radiat. Oncol., Biol., Phys.* **2004,** *59* (2), 21-26.

(13) Saeed, S.; Rashid, N.; Jones, P. G.; Ali, M.; Hussain, R., Synthesis, Characterization and Biological Evaluation of Some Thiourea Derivatives Bearing Benzothiazole Moiety as Potential Antimicrobial and Anticancer Agents. *Eur. J. Med. Chem.* **2010,** *45* (4), 1323-1331.

(14) Chang, H.; Sun, S.-Q., Silicon Nanoparticles: Preparation, Properties, and Applications. *Chinese Physics B* **2014,** *23* (8), 088102.

(15) Zhang, X.; Neiner, D.; Wang, S.; Louie, A. Y.; Kauzlarich, S. M., A New Solution Route to Hydrogen-Terminated Silicon Nanoparticles: Synthesis, Functionalization and Water Stability. *Nanotechnology* **2007,** *18* (9).

(16) Dasog, M.; Yang, Z.; Regli, S.; Atkins, T. M.; Faramus, A.; Singh, M. P.; Muthuswamy, E.; Kauzlarich, S. M.; Tilley, R. D.; Veinot, J. G. C., Chemical Insight into the Origin of Red and Blue Photoluminescence Arising from Freestanding Silicon Nanocrystals. *ACS Nano* **2013,** *7* (3), 2676-2685.

(17) Ledoux, G.; Guillois, O.; Porterat, D.; Reynaud, C.; Huisken, F.; Kohn, B.; Paillard, V., Photoluminescence Properties of Silicon Nanocrystals as a Function of Their Size. *Phys. Rev. B* **2000,** *62* (23), 15942-15951.

(18) Belomoin, G.; Therrien, J.; Smith, A.; Rao, S.; Twesten, R.; Chaieb, S.; Nayfeh, M. H.; Wagner, L.; Mitas, L., Observation of a Magic Discrete Family of Ultrabright Si Nanoparticles. *Appl. Phys. Lett.* **2002,** *80* (5), 841-843.

(19) English, D. S.; Pell, L. E.; Yu, Z.; Barbara, P. F.; Korgel, B. A., Size Tunable Visible Luminescence from Individual Organic Monolayer Stabilized Silicon Nanocrystal Quantum Dots. *Nano Lett.* **2002,** *2* (7), 681-685.

(20) Schuppler, S.; Friedman, S. L.; Marcus, M. A.; Adler, D. L.; Xie, Y. H.; Ross, F. M.; Chabal, Y. J.; Harris, T. D.; Brus, L. E.; Brown, W. L.; Chaban, E. E.; Szajowski, P. F.; Christman, S. B.; Citrin, P. H., Size, Shape, and Composition of Luminescent Species in Oxidized Si Nanocrystals and H-Passivated Porous Si. *Phys. Rev. B* **1995,** *52* (7), 4910-4925.

(21) Rogozhina, E.; Belomoin, G.; Smith, A.; Abuhassan, L.; Barry, N.; Akcakir, O.; Braun, P. V.; Nayfeh, M. H., Si--N Linkage in Ultrabright, Ultrasmall Si Nanoparticles. *Appl. Phys. Lett.* **2001,** *78* (23), 3711-3713.

(22) Rosso-Vasic, M.; Spruijt, E.; van Lagen, B.; De Cola, L.; Zuilhof, H., Alkyl-Functionalized Oxide-Free Silicon Nanoparticles: Synthesis and Optical Properties. *Small* **2008,** *4* (10), 1835-1841.

(23) Sato, S.; Swihart, M. T., Propionic-Acid-Terminated Silicon Nanoparticles: Synthesis and Optical Characterization. *Chem. Mater.* **2006,** *18* (17), 4083-4088.

(24) Fujioka, K.; Hiruoka, M.; Sato, K.; Manabe, N.; Miyasaka, R.; Hanada, S.; Hoshino, A.; Tilley, R. D.; Manome, Y.; Hirakuri, K.; Yamamoto, K., Luminescent Passive-Oxidized Silicon Quantum Dots as Biological Staining Labels and Their Cytotoxicity Effects at High Concentration. *Nanotechnology* **2008,** *19* (41), 415102.

(25) Zou, J.; Sanelle, P.; Pettigrew, K. A.; Kauzlarich, S. M., Size and Spectroscopy of Silicon Nanoparticles Prepared Via Reduction of Sicl4. *J. Cluster Sci.* **2006,** *17* (4), 565-578.

(26) Belomoin, G.; Therrien, J.; Nayfeh, M., Oxide and Hydrogen Capped Ultrasmall Blue Luminescent Si Nanoparticles. *Appl. Phys. Lett.* **2000,** *77* (6), 779-781.

(27) Chao, Y.; Šiller, L.; Krishnamurthy, S.; Coxon, P. R.; Bangert, U.; Gass, M.; Kjeldgaard, L.; Patoleo, S. N.; Lie, L. H.; O'Farrell, N.; Alsop, T. A.; Houlton, A.; Horrocks, B. R., Evaporation and Deposition of Alkyl-Capped Silicon Nanocrystals in Ultrahigh Vacuum. *Nat. Nanotechnol.* **2007,** *2* (8), 486-489.

(28) van Buuren, T.; Dinh, L. N.; Chase, L. L.; Siekhaus, W. J.; Terminello, L. J., Changes in the Electronic Properties of Si Nanocrystals as a Function of Particle Size. *Phys. Rev. Lett.* **1998,** *80* (17), 3803.

(29) Kobayashi, T.; Endoh, T.; Fukuda, H.; Nomura, S.; Sakai, A.; Ueda, Y., Ge Nanocrystals in Sio2 Films. *Appl. Phys. Lett.* **1997,** *71* (9), 1195-1197.

(30) Mangolini, L.; Thimsen, E.; Kortshagen, U., High-Yield Plasma Synthesis of Luminescent Silicon Nanocrystals. *Nano Lett.* **2005,** *5* (4), 655-659.

(31) Vial, J. C., Hot Papers - Physics - Mechanisms of Visible-Light Emission from Electro-Oxidized Porous Silicon by Vial,J.C., Bsiesy,A., Gaspard,F., Herino,R., Ligeon,M., Muller,F., Romestain,R., Macfarlane,R.M. *Scientist* **1994,** *8* (9), 16-16.

(32) Hata, K.; Yoshida, S.; Fujita, M.; Yasuda, S.; Makimura, T.; Murakami, K.; Shigekawa, H., Self-Assembled Monolayer as a Template to Deposit Silicon Nanoparticles Fabricated by Laser Ablation. *J. Phys. Chem. B* **2001,** *105* (44), 10842-10846.

(33) Bley, R. A.; Kauzlarich, S. M., A Low-Temperature Solution Phase Route for the Synthesis of Silicon Nanoclusters. *J. Am. Chem. Soc.* **1996,** *118* (49), 12461-12462.

(34) Wang, Q.; Ni, H.; Pietzsch, A.; Hennies, F.; Bao, Y.; Chao, Y., Synthesis of Water-Dispersible Photoluminescent Silicon Nanoparticles and Their Use in Biological Fluorescent Imaging. *J. Nanopart. Res.* **2011,** *13* (1), 405-413.

(35) Berridge, M. V.; Tan, A. S., Characterization of the Cellular Reduction of 3-(4,5-Dimethylthiazol-2-Yl)-2,5-Diphenyltetrazolium Bromide (Mtt) - Subcellular-Localization, Substrate Dependence, and Involvement of Mitochondrial Electron-Transport in Mtt Reduction. *Arch. Biochem. Biophys.* **1993,** *303* (2), 474-482.

(36) Wang, Q.; Bao, Y.; Ahire, J.; Chao, Y., Co-Encapsulation of Biodegradable Nanoparticles with Silicon Quantum Dots and Quercetin for Monitored Delivery. *Adv. Health. Mater.* **2013,** *2*, 459-465.

(37) Wu, H.; Liang, H.; Yuan, Q.; Wang, T.; Yan, X., Preparation and Stability Investigation of the Inclusion Complex of Sulforaphane with Hydroxypropyl-Beta-Cyclodextrin. *Carbohydr. Polym.* **2010,** *82* (3), 613-617.

(38) Medda, F.; Russell, R. J. M.; Higgins, M.; McCarthy, A. R.; Campbell, J.; Slawin, A. M. Z.; Lane, D. P.; Lain, S.; Westwood, N. J., Novel Cambinol Analogs as Sirtuin Inhibitors: Synthesis, Biological Evaluation, and Rationalization of Activity. *J. Med. Chem.* **2009,** *52* (9), 2673-2682.

(39) Pedras, M. S. C.; Zheng, Q.-A.; Gadagi, R. S., The First Naturally Occurring Aromatic Isothiocyanates, Rapalexins a and B, Are Cruciferous Phytoalexins. *Chem. Commun.* **2007,** (4), 368-370.

(40) Koca, I.; Ozgur, A.; Coskun, K. A.; Tutar, Y., Synthesis and Anticancer Activity of Acyl Thioureas Bearing Pyrazole Moiety. *Biorg. Med. Chem.* **2013,** *21* (13), 3859-3865.

(41) Wang, J.; Sun, S.; Peng, F.; Cao, L.; Sun, L., Efficient One-Pot Synthesis of Highly Photoluminescent Alkyl-Functionalised Silicon Nanocrystals. *Chem. Commun.* **2011,** *47* (17), 4941-4943.

(42) Mekki, A.; Holland, D.; McConville, C. F.; Salim, M., An Xps Study of Iron Sodium Silicate Glass Surfaces. *J. Non-Cryst. Solids* **1996,** *208* (3), 267-276.

(43) Du, H. H.; Tressler, R. E.; Spear, K. E.; Pantano, C. G., Oxidation Studies of Crystalline Cvd Silicon-Nitride. *J. Electrochem. Soc.* **1989,** *136* (5), 1527-1536.

(44) Chao, Y.; Wang, Q.; Pietzsch, A.; Hennies, F.; Ni, H., Soft X-Ray Induced Oxidation on Acrylic Acid Grafted Luminescent Silicon Quantum Dots in Ultrahigh Vacuum. *Phys. Status Solidi A-Appl. Mat.* **2011,** *208* (10), 2424-2429.

(45) Thompson, A.; Attwood, D.; Gullikson, E.; Howells, M.; Kim, K.-J.; Kirz, J.; Kortright, J.; Lindau, I.; Pianetta, P.; Robinson, A.; Scofield, J.; Vaughan, D.; Williams, G., *X-Ray Data Booklet*. Lawrence Berkeley National Lab: Berkeley, 2001.

(46) Barber, M.; Connor, J. A.; Guest, M. F.; Hillier, I. H.; Schwarz, M., Bonding in Some Donor-Acceptor Complexes Involving Boron-Trifluoride - Study by Means of Esca and Molecular-Orbital Calculations. *J. Chem. Soc., Faraday Trans. 2* **1973,** (4), 551-558.

(47) Dementjev, A. P.; de Graaf, A.; van de Sanden, M. C. M.; Maslakov, K. I.; Naumkin, A. V.; Serov, A. A., X-Ray Photoelectron Spectroscopy Reference Data for Identification of the C3n4 Phase in Carbon-Nitrogen Films. *Diamond Relat. Mater.* **2000,** *9* (11), 1904-1907.

(48) Fabrega, J.; Luoma, S. N.; Tyler, C. R.; Galloway, T. S.; Lead, J. R., Silver Nanoparticles: Behaviour and Effects in the Aquatic Environment. *Environment International* **2011,** *37* (2), 517-531.

(49) Williams, A. T. R.; Winfield, S. A.; Miller, J. N., Relative Fluorescence Quantum Yields Using a Computer-Controlled Luminescence Spectrometer. *Analyst* **1983,** *108* (1290), 1067-1071.

(50) Ahire, J. H.; Wang, Q.; Coxon, P. R.; Malhotra, G.; Brydson, R.; Chen, R.; Chao, Y., Highly Luminescent and Nontoxic Amine-Capped Nanoparticles from Porous Silicon: Synthesis and Their Use in Biomedical Imaging. *ACS Appl. Mater. Interfaces* **2012,** *4* (6), 3285-3292.

(51) Mozzi, A.; Forcella, M.; Riva, A.; Difrancesco, C.; Molinari, F.; Martin, V.; Papini, N.; Bernasconi, B.; Nonnis, S.; Tedeschi, G.; Mazzucchelli, L.; Monti, E.; Fusi, P.; Frattini, M., Neu3 Activity Enhances Egfr Activation without Affecting Egfr Expression and Acts on Its Sialylation Levels. *Glycobiology* **2015,** *25* (8), 855-868.

(52) Le Roy, C.; Wrana, J. L., Clathrin- and Non-Clathrin-Mediated Endocytic Regulation of Cell Signalling. *Nat. Rev. Mol. Cell Biol.* **2005,** *6* (2), 112-126.

(53) Björkelund, H.; Gedda, L.; Malmqvist, M.; Andersson, K., Resolving the Egf-Egfr Interaction Characteristics through a Multiple-Temperature, Multiple-Inhibitor, Real-Time Interaction Analysis Approach. *Mol. Clin. Oncol.* **2013,** *1* (2), 343-352.

(54) SiShi, L.; Buchbinder, E.; Wu, L.; Bjorge, J.; Fujita, D.; Zhu, S., Egfr and Her2 Levels Are Frequently Elevated in Colon Cancer Cells. *Discoveries Reports* **2014,** *1* (1), e1.

Graphic abstract: